

# Light-Induced Cation Exchange for Copper Sulfide Based CO<sub>2</sub> Reduction

Aurora Manzi,<sup>†,‡</sup> Thomas Simon,<sup>†,‡</sup> Clemens Sonnleitner,<sup>†,‡</sup> Markus Döblinger,<sup>||,‡</sup> Regina Wyrwich,<sup>||</sup> Omar Stern,<sup>§</sup> Jacek K. Stolarczyk,<sup>\*,†,‡</sup> and Jochen Feldmann<sup>†,‡</sup>

<sup>†</sup>Photonics and Optoelectronics Group, Department of Physics and Center for NanoScience (CeNS), Ludwig-Maximilians-Universität München, Amalienstr. 54, 80799 Munich, Germany

<sup>‡</sup>Nanosystems Initiative Munich (NIM), Schellingstr. 4, 80799 Munich, Germany

<sup>||</sup>Department of Chemistry, Ludwig-Maximilians-Universität München, Butenandtstr. 5-13 (E), 81377 Munich, Germany

<sup>§</sup>General Electric (GE) Global Research, Freisinger Landstr. 50, 85748 Garching bei München, Germany

## S Supporting Information

**ABSTRACT:** Copper(I)-based catalysts, such as Cu<sub>2</sub>S, are considered to be very promising materials for photocatalytic CO<sub>2</sub> reduction. A common synthesis route for Cu<sub>2</sub>S via cation exchange from CdS nanocrystals requires Cu(I) precursors, organic solvents, and neutral atmosphere, but these conditions are not compatible with *in situ* applications in photocatalysis. Here we propose a novel cation exchange reaction that takes advantage of the reducing potential of photoexcited electrons in the conduction band of CdS and proceeds with Cu(II) precursors in an aqueous environment and under aerobic conditions. We show that the synthesized Cu<sub>2</sub>S photocatalyst can be efficiently used for the reduction of CO<sub>2</sub> to carbon monoxide and methane, achieving formation rates of 3.02 and 0.13 μmol h<sup>-1</sup> g<sup>-1</sup>, respectively, and suppressing competing water reduction. The process opens new pathways for the preparation of new efficient photocatalysts from readily available nanostructured templates.

Fossil fuels play a pivotal role in the energy supply and production, meeting more than 80% of the global demand. Nonetheless, the use of this finite and exhaustible source is invariably linked with carbon dioxide emission. One sustainable approach to mitigate the effects of the emission is to close the carbon cycle by producing fuels, e.g., methane, again from CO<sub>2</sub>, where the energy required to drive the uphill CO<sub>2</sub> reduction reaction would come from solar irradiation.<sup>1</sup> In addition, this approach ensures convenient storage capability of the harvested solar energy.

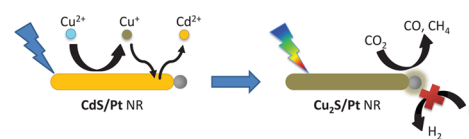
The heterostructures composed of colloidal semiconductor nanocrystals and metal or metal oxide co-catalysts have attracted a lot of attention in the field of photocatalytic CO<sub>2</sub> reduction, owing to the advances in their fabrication and favorable optoelectronic and catalytic properties.<sup>2</sup> Although CO<sub>2</sub> is a highly stable molecule and its reduction is a complex multi-electron- multiproton- transfer process, copper-based catalysts are considered the most promising candidates for achieving good conversion efficiency. This is due to their strongly reducing conduction band and selectivity toward CO<sub>2</sub> rather than

competing water reduction.<sup>3</sup> Copper(I) sulfide, Cu<sub>2</sub>S, a narrow (1.2 eV) indirect band gap p-type semiconductor is of particular interest because it can act as both light absorber and co-catalyst<sup>4</sup> and has been shown to reduce CO<sub>2</sub>.<sup>5</sup> The band gap width can be tuned upward by introducing copper vacancies. This leads to nonstoichiometric direct band gap Cu<sub>2-x</sub>S, which additionally exhibits plasmonic resonance in the near-infrared (NIR) region.<sup>6,7</sup> This direct synthesis of Cu<sub>2</sub>S with controlled nanometric properties is, however, not easily achieved and usually takes place in organic solvents<sup>8</sup> or requires controlled atmosphere and Cu(I) precursors.<sup>9</sup>

An alternative approach to fabricate ionic nanocrystals such as Cu<sub>2</sub>S is to use the cation exchange technique that, starting from a well-defined structure of one material, leads to the desired material by substituting the initial cationic sublattice with a different one by keeping the initial geometrical structure.<sup>10</sup> It is then possible to take advantage of the controlled geometrical properties of nanocrystals such as CdS that are synthesized via hot-injection techniques and use them as scaffolds for new materials. This technique has been used to create Cu<sub>2</sub>S nanostructures from CdS.<sup>11</sup> Unfortunately, the standard procedure has several limitations that are not compatible with *in situ* preparation of a photocatalytic material, such as the necessity to be performed in a controlled atmosphere and in organic solvents.

Here we present a novel cation exchange method in which we harness the reducing potential of photoexcited electrons in the conduction band of CdS nanocrystals to fabricate copper-deficient Cu<sub>2-x</sub>S nanorods (NRs) from CdS using Cu<sup>2+</sup> precursors (cf. Scheme 1). In contrast to other cation exchange methods, this photoinduced process can proceed under aerobic

## Scheme 1. Light-Induced Cation Exchange Leading to Photocatalytic CO<sub>2</sub> Reduction into CO and CH<sub>4</sub>



Received: June 30, 2015

Published: October 19, 2015

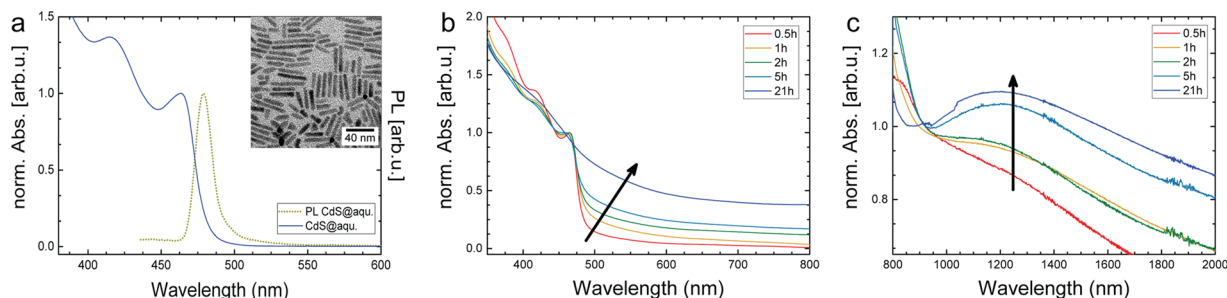


**Figure 1.** (a) Absorbance (left axis) and PL (right axis) spectra of CdS NRs in aqueous solution, excitation wavelength 420 nm, arbitrary units. Inset in (a) shows a TEM image of the CdS NRs. Absorbance in the (b) UV–vis and (c) IR regions of CdS NRs during the cation exchange with Cu cations at various illumination times, arbitrary units.

conditions, yet preserves the shape of the original crystals and enables complete conversion of CdS to copper sulfide. We further demonstrate that the as-prepared  $\text{Cu}_2\text{S}$  NRs can be used *in situ* as an efficient photocatalyst for reducing  $\text{CO}_2$  to carbon monoxide and methane with excellent selectivity over hydrogen production.

**Results and Discussion.** The CdS NRs were synthesized according to a previously published procedure<sup>12</sup> and were subsequently transferred into an aqueous environment using L-cysteine as a stabilizing ligand. Their absorption spectrum exhibited a distinct excitonic peak at 463 nm with sharp absorption onset (Figure 1a). The band-edge photoluminescence (PL) peak was located around 480 nm. On the basis of the analysis of TEM images (e.g., Figure 1a inset), the NRs were on average 30 nm in length and 5 nm in width.

The cation exchange from divalent  $\text{Cd}^{2+}$  cations to monovalent  $\text{Cu}^+$  cations was performed by illuminating under air a dispersion of CdS NRs in water with a 447 nm laser in the presence of Cu(II) precursor ( $\text{CuCl}_2$ ) and triethanolamine (TEOA) as a hole scavenger. Further details are provided in the Supporting Information (SI). Over the course of the illumination we observed that the excitonic peaks of CdS became broader and gradually disappeared altogether after 21 h (cf. Figure 1b). At the same time, the absorption in the range 500–800 nm was increased in comparison with the original CdS dispersion. Meanwhile, in the NIR region (Figure 1c) a broad peak arose around 1200 nm that could be identified as a plasmonic resonance characteristic of nonstoichiometric copper sulfide  $\text{Cu}_{2-x}\text{S}$  nanostructures.<sup>6,13</sup>

In order to further characterize the evolution of the system high-resolution TEM and high-angle annular dark-field (HAADF) STEM images were acquired at 0.5, 2.5, and 25 h of illumination. At the early stage (Figure 2a), the CdS wurtzite structure of the NRs was still clearly visible. After 2.5 h, this crystal structure could be identified only in few selected areas, although the shape of the NR was fully preserved (cf. Figures 2b and S1). At this intermediate stage the binary CdS and  $\text{Cu}_2\text{S}$  phases coexist, separated mostly by interfaces perpendicular to the long axis of the NR (Figures S2 and S3). This is in agreement with earlier reports on CdS- $\text{Cu}_2\text{S}$  system.<sup>11</sup> The images and elemental mapping (Figure S4) show that the  $\text{Cu}_2\text{S}$  domains grow at the expense of CdS domains. The CdS domains were not observed anymore after 25 h of illumination (cf. Figure 2c), indicating a complete cation exchange. The electron diffraction patterns (Figure S5) and the most prominent lattice planes in HR-TEM images (Figure S6) are consistent with the high-chalcocite phase of copper sulfide.

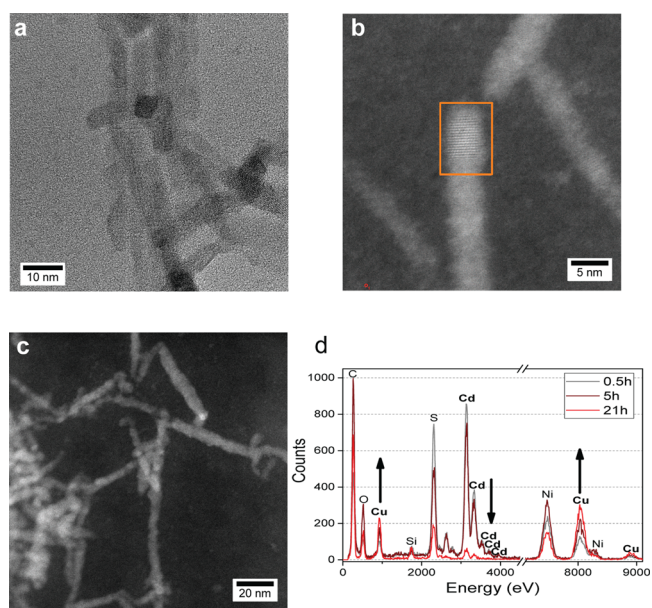


**Figure 2.** (a) HR-TEM images of CdS NRs after 0.5 h of light-induced cation exchange with Cu. HAADF STEM images of CdS NRs after (b) 2.5 and (c) 25 h of light-induced cation exchange with Cu. The orange box in (b) shows a NR region having wurtzite-type stacking with a layer distance of 0.34 nm that can be identified with CdS. (d) EDX measurements on CdS NRs at different stages of cation exchange.

The confirmation that these changes in the crystallographic structure correspond indeed to changes in composition due to the cation exchange process was obtained by energy dispersive X-ray (EDX) spectroscopy (Figures 2d and S2). After 30 min of illumination, the ratio of Cd:S was 1:1, as expected for a sample composed mainly of CdS (Table S1). At this early stage, the ratio Cu:S was 1:6, indicating only minor inclusion of copper. After 21 h, the proportions more than reversed. The ratio Cd:S decreased to 1:6, confirming the depletion of cadmium from the NRs, whereas the ratio of Cu to S rose to almost 2:1 (1.82:1). The implied formation of nearly stoichiometric  $\text{Cu}_2\text{S}$  is in good agreement with plasmonic features observed in the NIR absorption spectrum (cf. Figure 1c).

The changes in the NR composition during the cation exchange were further analyzed by inductively coupled plasma atomic emission spectroscopy (ICP-AES, see Figure S7). The results corroborate our findings, showing that during the process the amount of Cd decreased in the NRs but increased in the solution, while the opposite trends were observed for Cu.

The sample which had been illuminated for 24 h was also analyzed by X-ray photoelectron spectroscopy (XPS) before and

after argon sputtering. The latter process has an effect of removing the outer nanometer-thick layer of the material. While the amount of Cu was nearly the same before and after sputtering, the amount of Cd decreased significantly after sputtering (Figure S8). This confirms that only traces of Cd were located inside of the NRs at the end of the illumination.

The control experiments performed in the dark for over 75 h showed no changes to the absorption spectrum of the CdS NRs (Figure S9). Clearly, without the incident photon flux, the  $\text{Cu}^{2+}$  ions cannot be incorporated into the CdS lattice to induce the changes observed under 447 nm laser illumination. This laser wavelength was chosen to ensure strong absorption by the CdS NRs. Upon absorption of a photon with such energy, i.e., above the band gap, an electron is excited to the conduction band. CdS is well-known to possess a strongly reducing conduction band (band edge potential at pH 7 equals  $-0.85$  V versus NHE),<sup>14</sup> capable of, e.g., reducing water to hydrogen. The standard redox potential of the couple  $\text{Cu}^{2+}/\text{Cu}^+$  is even lower ( $+0.15$  V) than of  $\text{H}^+/\text{H}_2$ , therefore we propose that the photogenerated electrons in CdS reduce  $\text{Cu}^{2+}$  to  $\text{Cu}^+$  before the latter cations exchange with  $\text{Cd}^{2+}$  in the CdS nanocrystal. Accordingly, this process is not dependent on the shape of the nanocrystal involved and only relies on the alignment of its conduction band. This is a similar process to deposition of Pt or Ni clusters on CdS by reduction of their respective cations by photoexcited electrons.<sup>14–16</sup> It could be argued that the substantial energy gain of incorporating  $\text{Cu}^+$  into the lattice<sup>10</sup> prevents further reduction of  $\text{Cu}^+$  to  $\text{Cu}(0)$ . The exchange reaction typically requires  $\text{Cu}^+$  precursors and a protective atmosphere to prevent oxidation.<sup>11</sup> The reducing environment provided by photoexcited CdS in the reported herein procedure makes these limitations unnecessary.

Moreover, under blue-light illumination, the CdS NRs would be expected, even without co-catalysts, to photocatalytically reduce water to hydrogen with low but measurable efficiency. Interestingly, we have not observed any  $\text{H}_2$  generation in the presence of Cu precursors, suggesting that the photogenerated electrons are indeed not used in this way. At the same time, the charge recombination is limited by the collection of the photogenerated hole by the scavenger (TEOA or  $\text{Na}_2\text{SO}_3$ ). It appears therefore that in the reported photoinduced cation exchange process, the CdS NRs serve not only as a scaffold for the formation of  $\text{Cu}_2\text{S}$  NRs but also as a photoactivated reducing agent for  $\text{Cu}^{2+}$  cations. In the intermediate stages of the cation exchange, both semiconductors, CdS and  $\text{Cu}_2\text{S}$ , coexist and form a type II band alignment. Photon absorption by either of them enables the exchange reaction because the electron photoexcited in  $\text{Cu}_2\text{S}$  is expected to transfer to CdS and still be available for reducing  $\text{Cu}^{2+}$ .

The decoration of semiconductor nanocrystals with noble metal (e.g., Pt) co-catalyst nanoparticles (NPs) is a common approach in photocatalytic systems partially because the NPs act as sinks for photogenerated electrons and thereby improve the charge separation.<sup>17</sup> In this context, we decorated the CdS NRs with Pt NPs by two methods: a selective growth at the tips<sup>17,18</sup> or a random placement of multiple NPs on the NR surface by photodeposition.<sup>16</sup> The resulting heterostructures are shown in Figure S10a,b, respectively. For the decorated NRs the cation exchange process led to analogous products to the bare CdS rods (cf. Figures 3a and S2–S6). This is because the energy alignment (Figure 3b) would lead to a similar charge-transfer mechanism, with Pt NPs able to accumulate electrons and facilitate charge separation.

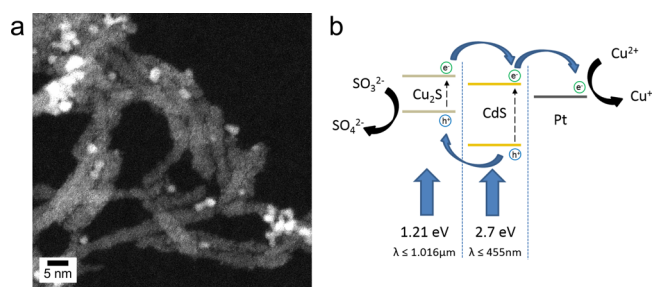


**Figure 3.** (a) HAADF STEM image of CdS NRs randomly decorated with Pt after 21 h of light-induced cation exchange with Cu. (b) Schematic of the energy band alignment in the studied system.

The as-prepared  $\text{Cu}_2\text{S}$ –Pt nanostructures were tested in *in situ* photocatalytic  $\text{CO}_2$  reduction experiments.  $\text{Na}_2\text{CO}_3$  was used as carbon source, and  $\text{Na}_2\text{SO}_3$  was used as a hole scavenger. The carbon-free scavenger was chosen in order to make sure that the putative  $\text{CO}_2$  reduction products do not originate from the decomposition of the scavenger. The whole process, from the cation exchange to the  $\text{CO}_2$  reduction, was performed in special quartz cuvettes equipped with a side neck with a screw cap and a septum to enable collection of the headspace for analysis in a GC-MS setup (Figure S11). The cuvettes were flushed with helium for compatibility with the instrument. The reduction of  $\text{O}_2$  can compete with the  $\text{Cu}^{2+}$  reduction, thus in its absence the cation exchange was slightly faster (Figure S12). A more detailed description of the photocatalytic experiments is given in the SI.

Carbon monoxide (CO) evolution was observed for 90 h from the system decorated with Pt on tips during the  $30 \text{ mW cm}^{-2}$  illumination with a 447 nm blue laser with a formation rate  $R = 31.04 \text{ nmol h}^{-1} \text{ g}^{-1}$  (Figure 4a). Interestingly, these measure-

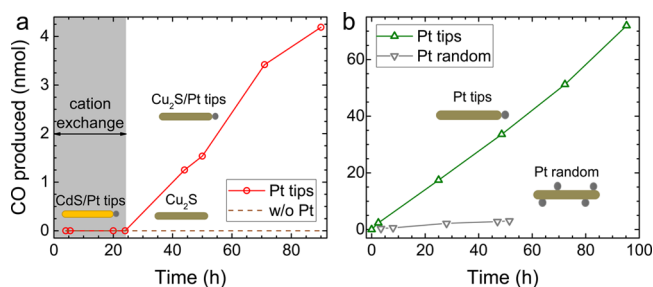


**Figure 4.** CO evolution from CdS– $\text{Cu}_2\text{S}$  NRs after illumination with (a) a 447 nm laser or (b) a broad spectrum Xe lamp.

ments showed an activation time for CO production of 24 h that perfectly matches with the time required for the completion of the cation exchange that was identified to be around 25 h. During the exchange the photogenerated electrons are used for reducing  $\text{Cu}^{2+}$  instead of  $\text{CO}_2$ . Indeed, excess  $\text{Cu}^{2+}$  slows down the reaction (Figure S13). In addition, the  $\text{Cu}_2\text{S}$  phase is needed to reduce  $\text{CO}_2$ , since a control experiment performed without the presence of Cu precursors (with or without Pt NPs) did not show any evolution of  $\text{CO}_2$  reduction products. Interestingly, both the bare CdS NRs and the NRs with randomly photodeposited Pt NPs did not lead to any gas evolution. The latter result likely stems from a faster recombination rate in these structures due to a less effective charge separation.<sup>17</sup>

Under broad-spectrum illumination with a Xe lamp with a cutoff water filter for the IR wavelengths the CO formation rates were significantly higher,  $39.48 \text{ nmol h}^{-1} \text{ g}^{-1}$  for the NRs randomly decorated with Pt and  $3.02 \mu\text{mol h}^{-1} \text{ g}^{-1}$  for the tip-



decorated NRs, respectively (Figure 4b). The cation exchange is much faster in this case (cf. Figure S14 and Tables S1 vs S2), which leads to a shorter activation time. While the illumination was stronger, this underlines the impact of the broad absorption of the visible light by Cu<sub>2</sub>S. Methane evolution was also observed using Xe lamp illumination for the tip-decorated sample, albeit with much smaller formation rate 0.13 μmol h<sup>-1</sup> g<sup>-1</sup> than what was measured for CO (cf. Figure S15). This reflects the much more complex 8-electron pathway to generation of CH<sub>4</sub> from CO<sub>2</sub>, in comparison with a far simpler 2-electron process for CO.<sup>2</sup>

We have not detected any H<sub>2</sub> evolution from the sample at any stage of the illumination by either source. This might appear surprising at first because the CdS-Pt system is a known good photocatalyst for H<sub>2</sub> production.<sup>16,17</sup> The noted selectivity toward CO<sub>2</sub> reduction, associated with Cu-based catalysts, likely arises from the formation of a thin copper-based shell around the Pt NPs which inhibits the reduction of H<sup>+</sup>, as indicated by the HAADF-STEM analysis (Figure S16). A similar effect was demonstrated previously by Zhai et al. for TiO<sub>2</sub> particles decorated with Pt/Cu<sub>2</sub>O core/shell NPs.<sup>19</sup> The overgrowth of the Pt NPs with a thin shell can also be inferred from the XPS measurements which show an increase of Pt concentration after removing of the surface layers of the photocatalyst by ion sputtering (Figure S17).

The control experiments using band-pass filters to select only the wavelengths longer than 570 nm, which still show CO and CH<sub>4</sub> production, prove that the CO<sub>2</sub> reduction should not be attributed to the original CdS NRs but instead to the produced Cu<sub>2</sub>S NRs (see Figure S18). Only traces of products detected in further experiments without a carbon source confirm that CO and CH<sub>4</sub> indeed originate from the reduction of CO<sub>2</sub> (see Figure S19).

In summary, we report a novel light-induced cation exchange for the formation of Cu<sub>2</sub>S NRs from CdS NRs, although its general character renders it applicable also to other nanostructures. Owing to the reducing character of the photoexcited electron in CdS conduction band, the reaction can be performed in aqueous medium without protective atmosphere and can use Cu<sup>2+</sup> in solution as copper ion source. The nonrestrictive conditions of the process are perfectly compatible with the solar fuel generating photocatalytic reactions and open possible new pathways for preparation of other ionic photocatalysts. We have demonstrated that the formed copper sulfide NRs can be used as an efficient catalyst for CO<sub>2</sub> reduction to CO and CH<sub>4</sub> under broad visible light illumination with high selectivity with respect to water reduction.

## ■ ASSOCIATED CONTENT

### 📄 Supporting Information

The Supporting Information is available free of charge on the ACS Publications website at DOI: 10.1021/jacs.5b06778.

Experimental procedures and additional data (PDF)

## ■ AUTHOR INFORMATION

### Corresponding Author

\*jacek.stolarczyk@physik.uni-muenchen.de

### Notes

The authors declare no competing financial interest.

## ■ ACKNOWLEDGMENTS

This work was supported by the Bavarian State Ministry of Science, Research, and Arts through the grant “Solar Technologies go Hybrid (SolTech)” and by General Electric (GE) Global Research. The authors thank Jaroslava Obel for the ICP-AES measurements.

## ■ REFERENCES

- (1) Olah, G. A.; Prakash, G. K. S.; Goepfert, A. *J. Am. Chem. Soc.* **2011**, *133*, 12881.
- (2) Habisreutinger, S. N.; Schmidt-Mende, L.; Stolarczyk, J. K. *Angew. Chem., Int. Ed.* **2013**, *52*, 7372.
- (3) (a) Peterson, A. A.; Abild-Pedersen, F.; Studt, F.; Rossmeisl, J.; Nørskov, J. K. *Energy Environ. Sci.* **2010**, *3*, 1311; (b) Neațu, S.; Maciá-Agulló, J. A.; Concepción, P.; Garcia, H. *J. Am. Chem. Soc.* **2014**, *136*, 15969; (c) Yin, G.; Nishikawa, M.; Nosaka, Y.; Srinivasan, N.; Atarashi, D.; Sakai, E. *ACS Nano* **2015**, *9*, 2111; (d) An, X.; Li, K.; Tang, J. *ChemSusChem* **2014**, *7*, 1086.
- (4) Wu, Y.; Wadia, C.; Ma, W.; Sadtler, B.; Alivisatos, A. P. *Nano Lett.* **2008**, *8*, 2551.
- (5) Kar, P.; Farsinezhad, S.; Zhang, X.; Shankar, K. *Nanoscale* **2014**, *6*, 14305.
- (6) Zhao, Y.; Pan, H.; Lou, Y.; Qiu, X.; Zhu, J.; Burda, C. *J. Am. Chem. Soc.* **2009**, *131*, 4253.
- (7) Kriegel, I.; Jiang, C.; Rodríguez-Fernández, J.; Schaller, R. D.; Talapin, D. V.; da Como, E.; Feldmann, J. *J. Am. Chem. Soc.* **2012**, *134*, 1583.
- (8) (a) Sigman, M. B.; Ghezelbash, A.; Hanrath, T.; Saunders, A. E.; Lee, F.; Korgel, B. A. *J. Am. Chem. Soc.* **2003**, *125*, 16050; (b) Zhuang, Z.; Peng, Q.; Zhang, B.; Li, Y. *J. Am. Chem. Soc.* **2008**, *130*, 10482; (c) Du, X.-S.; Mo, M.; Zheng, R.; Lim, S.-H.; Meng, Y.; Mai, Y.-W. *Cryst. Growth Des.* **2008**, *8*, 2032.
- (9) Ma, G.; Zhou, Y.; Li, X.; Sun, K.; Liu, S.; Hu, J.; Kotov, N. A. *ACS Nano* **2013**, *7*, 9010.
- (10) (a) Rivest, J. B.; Jain, P. K. *Chem. Soc. Rev.* **2013**, *42*, 89; (b) Jain, P. K.; Amirav, L.; Aloni, S.; Alivisatos, A. P. *J. Am. Chem. Soc.* **2010**, *132*, 9997; (c) Beberwyck, B. J.; Surendranath, Y.; Alivisatos, A. P. *J. Phys. Chem. C* **2013**, *117*, 19759.
- (11) (a) Sadtler, B.; Demchenko, D. O.; Zheng, H.; Hughes, S. M.; Merkle, M. G.; Dahmen, U.; Wang, L.-W.; Alivisatos, A. P. *J. Am. Chem. Soc.* **2009**, *131*, 5285; (b) Plante, I. J.-L.; Teitelboim, A.; Pinkas, I.; Oron, D.; Mokari, T. *J. Phys. Chem. Lett.* **2014**, *5*, 590.
- (12) Saunders, A. E.; Ghezelbash, A.; Sood, P.; Korgel, B. A. *Langmuir* **2008**, *24*, 9043.
- (13) Kriegel, I.; Rodríguez-Fernández, J.; Wisnet, A.; Zhang, H.; Waurisch, C.; Eychmüller, A.; Dubavik, A.; Govorov, A. O.; Feldmann, J. *ACS Nano* **2013**, *7*, 4367.
- (14) Simon, T.; Bouchonville, N.; Berr, M. J.; Vaneski, A.; Adrović, A.; Volbers, D.; Wyrwich, R.; Döblinger, M.; Susha, A. S.; Rogach, A. L.; Jäckel, F.; Stolarczyk, J. K.; Feldmann, J. *Nat. Mater.* **2014**, *13*, 1013.
- (15) Dukovic, G.; Merkle, M. G.; Nelson, J. H.; Hughes, S. M.; Alivisatos, A. P. *Adv. Mater.* **2008**, *20*, 4306.
- (16) Berr, M.; Vaneski, A.; Susha, A. S.; Rodríguez-Fernández, J.; Döblinger, M.; Jäckel, F.; Rogach, A. L.; Feldmann, J. *Appl. Phys. Lett.* **2010**, *97*, 093108.
- (17) (a) Amirav, L.; Alivisatos, A. P. *J. Phys. Chem. Lett.* **2010**, *1*, 1051; (b) Wu, K.; Chen, Z.; Lv, H.; Zhu, H.; Hill, C. L.; Lian, T. *J. Am. Chem. Soc.* **2014**, *136*, 7708.
- (18) Habas, S. E.; Yang, P.; Mokari, T. *J. Am. Chem. Soc.* **2008**, *130*, 3294.
- (19) Zhai, Q.; Xie, S.; Fan, W.; Zhang, Q.; Wang, Y.; Deng, W.; Wang, Y. *Angew. Chem., Int. Ed.* **2013**, *52*, 5776.